E11-2017-68

M. B. Yuldasheva, O. I. Yuldashev

APPLICATION OF HARMONIC BASIS OF A HIGH ORDER FOR SOLVING SOME MAGNETOSTATIC PROBLEMS

Submitted to “Computational Mathematics and Modeling”

Юлдашева М. Б., Юлдашев О. И. E11-2017-68

Применение гармонического базиса высокого порядка для решения некоторых задач магнитостатики

Целью работы является исследование возможностей использования гармонического базиса высокого порядка аппроксимации для решения некоторых задач магнитостатики. Мы рассматриваем известные методы с нашим базисом и ранее разработанный нами подход. В работе представлены численные результаты сравнения этих методов при решении линейной задачи на последовательностях сеток с различными параметрами h и p. Для нелинейной задачи относительно двух скалярных потенциалов показано, что эта модель в новой предлагаемой слабой формулировке сохраняет свойство монотонности. По результатам работы можно сделать вывод, что гармонический базис дает более точные приближенные решения на адаптивных сетках для рассмотренных задач магнитостатики по сравнению с обычным подходом.

Работа выполнена в Лаборатории информационных технологий ОИЯИ.

Препринт Объединенного института ядерных исследований. Дубна, 2017

Yuldasheva M. B., Yuldashev O. I. E11-2017-68

Application of Harmonic Basis of a High Order for Solving Some Magnetostatic Problems

The aim of this work is investigation of possibilities of using high-order harmonic basis for solving some magnetostatic problems. We consider known methods with our basis and the approach earlier elaborated by the authors. We present numerical results of their comparison when solving a linear problem on sequences of meshes with various parameters h and p. For a nonlinear problem with respect to two scalar potentials, it is shown that this model, in the suggested new weak formulation, keeps the property of monotonicity. From the results of this work it may be concluded that the harmonic basis gives more exact approximations on adaptive meshes for the considered magnetostatic problems in comparison with the usual approach.

The investigation has been performed at the Laboratory of Information Technologies, JINR.

Preprint of the Joint Institute for Nuclear Research. Dubna, 2017

1. INTRODUCTION

Magnetic fields have broad application and play an important role in scientific research of the structure of matter. Homogeneity of stationary magnetic fields in electromagnets of accelerators is characterized by coefficients of their expansion in a series on harmonic functions [1]. From there was an idea to find magnetic fields by means of harmonic basis with approximation of a high order using discontinuous projection methods. Usual computer models of electromagnets may generate vertex and edge singularities in approximate solutions. It is also the reason for finding an optimal basis for an optimal adaptive discretization.

The paper is organized as follows. In Section 2 the formulations of nonlinear and linear magnetostatic problems are given. Section 3 deals with the methods in which harmonic basis can be used. Section 4 presents comparison of these methods with the usual continuous Galerkin method of a high order. In Section 5 the harmonic basis is applied for solving nonlinear magnetostatics problems in the formulation for the total and reduced scalar potentials. Here, the new weak formulation, developed by the authors, is used.

2. FORMULATIONS OF MAGNETOSTATIC PROBLEMS

Consider the problem of magnetostatics with respect to the total $\varphi^{(1)}$ and reduced $\varphi^{(2)}$ scalar potentials in an area $\overline{\Omega} = \overline{\Omega}^{(1)} \cup \overline{\Omega}^{(2)}$. On smooth parts of the boundary define mutually orthogonal unit tangent, binormal, and normal vectors so that they make up a local right-handed Cartesian coordinate system. Denote these vectors by $\mathbf{s}$, $\mathbf{t}$, and $\mathbf{n}$, respectively. Define the vector function $\mathbf{u}_\tau = \mathbf{s}u_s + \mathbf{t}u_t$ with components u_s and u_t. With the notation we have the following problem [2]:

$$\begin{gathered}
\nabla \cdot (\mu^{(1)} \nabla \varphi^{(1)}) = 0, \quad x \in \Omega^{(1)}, \quad \nabla \cdot (\mu^{(2)} \nabla \varphi^{(2)}) = 0, \quad x \in \Omega^{(2)}, \\
\varphi^{(1)} = \varphi^{(2)} + \varphi^S, \quad \mu^{(1)} \partial \varphi^{(1)} / \partial n = \mu^{(2)} (\partial \varphi^{(2)} / \partial n + H_n^S), \\
\nabla_\tau \varphi^{(1)} = \nabla_\tau \varphi^{(2)} + \mathbf{H}_\tau^S, \quad x \in \Gamma,
\end{gathered} \tag{1}$$

$$\varphi^{(k)} = 0, \quad x \in \Gamma_D^{(k)}, \quad \mu^{(k)} \partial\varphi^{(k)}/\partial n = 0, \quad x \in \Gamma_N^{(k)}, \quad k = 1, 2.$$

Here, $\Omega^{(1)}$ and $\Omega^{(2)}$ are regions of ferromagnetic and nonmagnetic media, respectively; $\Gamma = (\partial\Omega^{(1)} \setminus (\Gamma_D^{(1)} \cup \Gamma_N^{(1)})) \cap (\partial\Omega^{(2)} \setminus (\Gamma_D^{(2)} \cup \Gamma_N^{(2)}))$, where $\Gamma_D^{(k)}$, $\Gamma_N^{(k)}$ are boundaries with the Dirichlet and Neumann conditions in these regions; $\Gamma_D^{(k)} \cap \Gamma = \emptyset$, $\Gamma_N^{(k)} \cap \Gamma = \emptyset$, $\nabla_\tau \varphi^{(k)} = \mathbf{s}\partial\varphi^{(k)}/\partial s + \mathbf{t}\partial\varphi^{(k)}/\partial t$, $k = 1, 2$; $\mu^{(1)} = \mu_0 \cdot \mu_r(|\nabla\varphi^{(1)}|)$ is a given continuously differentiable function, $\mu^{(2)} = \mu_0 > 0$, H_n^S, $\mathbf{H}_\tau^S$ are normal component and tangential vector of the given field $\mathbf{H}^S$, which is calculated by the Biot–Savart law:

$$\mathbf{H}^S(x) = \int\limits_{\Omega_S} \mathbf{J} \times \mathbf{V}^*(x, y)\, d\Omega_y,$$

where $\Omega_S \in \Omega^{(2)}$, $\mathbf{J}$ is a given vector function, $\mathbf{V}^*(x, y) = \nabla_y(1/(4\pi|x - y|))$ and $|x - y|$ is the distance between the points x and y. Note that the function φ^S is either calculated by the formula [2]

$$\varphi^S(x) = \varphi^S(y) - \int\limits_x^y \mathbf{H}_\tau^S \cdot d\tau, \quad x, y \in \Gamma,$$

where $\varphi^S(x_0) = \varphi_0^S$ is the value prescribed at the point $x_0 \in \Gamma$, or found by solving the problem [3]

$$\int\limits_\Gamma \nabla_\tau \varphi^S \cdot \nabla_\tau v dS = \int\limits_\Gamma \mathbf{H}_\tau^S \cdot \nabla_\tau v dS, \quad \varphi^S(x_0) = \varphi_0^S,$$

where v is a basis function. Note that the second formula does not accumulate errors in calculation of the vector $\mathbf{H}^S$ by means of cubature formulas in 3D. $\mathbf{B} = \mu^{(1)}\nabla\varphi^{(1)}$, $x \in \Omega^{(1)}$, or $\mathbf{B} = \mu^{(2)}\nabla\varphi^{(2)} + \mu^{(2)}\mathbf{H}^S$, $x \in \Omega^{(2)}$, is a magnetic flux density. In Section 5 we suggest a new weak formulation to solve (1) with high-order harmonic basis.

For the linear case we will consider the following problem with respect to unknown vectors $\mathbf{H}$ and $\mathbf{B}$:

$$\nabla \cdot \mathbf{B} = g, \quad \nabla \times \mathbf{H} = \mathbf{G}, \quad x \in \Omega; \tag{2}$$

$$\mathbf{n} \times \mathbf{H} = \mathbf{n} \times \mathbf{H}^*, \quad x \in \Gamma_D; \quad \mathbf{n} \cdot \mathbf{B} = \mathbf{n} \cdot \mathbf{B}^*, \quad x \in \Gamma_N.$$

Here, g and $\mathbf{G}$ are given, $\nabla \cdot \mathbf{G} = 0$, $\mathbf{n}$ is an external normal vector to Ω, $\partial\Omega = \overline{\Gamma}_D \cup \overline{\Gamma}_N$, $\Gamma_D \cap \Gamma_N = \emptyset$, $\Gamma_D \neq \emptyset$. Taking into account that $\mathbf{B} = \mu_0\mathbf{H}$, problem (2) is reduced to the linear div-curl system relative to $\mathbf{H}$ with $\tilde{g} = g/\mu_0$. In Section 3 we consider some methods for solving this system with high-order harmonic basis.

3. METHODS WITH HARMONIC BASIS OF A HIGH ORDER

For solving problems (1) and (2) with high-order harmonic basis, one can use the integral equation method [4], the least square method [5] or the discontinuous Galerkin method [6].

3.1. Formulations. Let us introduce some notation for short description of these approaches. Let T_h be a regular partition [7] of the region Ω and $\Gamma_{\rm int}$ be the interior boundary between cells:

$$\overline{\Omega} = \bigcup_{k=1}^{N(P_h)} \overline{\Omega}_k, \;\; \Omega_k \cap \Omega_l = \emptyset, \;\; \Gamma_{\rm int} = \bigcup_{\Omega_k, \Omega_l \in P_h} \Gamma_{kl}, \;\; \Gamma_{kl} = \partial\Omega_k \cap \partial\Omega_l, \;\; k \neq l.$$

By $[\![\cdot]\!]$ and $\{\{\cdot\}\}$ we denote the jump and the average of function across the boundary between two cells, respectively:

$$[\![\mathbf{u}]\!]|_{\Gamma_{kl} \in \Gamma_{\rm int}} = \mathbf{u}|_{\partial\Omega_k} - \mathbf{u}|_{\partial\Omega_l}, \quad k < l;$$

$$\{\{\mathbf{u}\}\}|_{\Gamma_{kl} \in \Gamma_{\rm int}} = (\mathbf{u}|_{\partial\Omega_k} + \mathbf{u}|_{\partial\Omega_l})/2, \quad k \neq l.$$

For cells with $\Gamma_k \subset \Gamma_D$ we define

$$[\![\mathbf{u}]\!]|_{\Gamma_k \subset \Gamma_D} = \mathbf{u}|_{\partial\Omega_k}, \quad \{\{\mathbf{u}\}\}|_{\Gamma_k \subset \Gamma_D} = \mathbf{u}|_{\partial\Omega_k}.$$

Here, $\mathbf{u}|_{\partial\Omega_k}$ and $\mathbf{u}|_{\partial\Omega_l}$ are the traces of vector functions $\mathbf{u}|_{\Omega_k}$, $\mathbf{u}|_{\Omega_l}$. As a normal vector on the common boundary Γ_{kl} between adjacent cells Ω_k and Ω_l, we use an external normal vector to Ω_k, if $k < l$.

Assume that in $\Omega_k \subset T_h$ the approximate solution has the form [8]

$$\mathbf{H} = \nabla\varphi + \mathbf{w}, \tag{3}$$

where φ is a harmonic function and $\mathbf{w}$ is a particular solution:

$$\nabla \cdot \mathbf{w} = \tilde{g}, \quad \nabla \times \mathbf{w} = \mathbf{G}, \quad x \in \Omega_k.$$

For problem (2), when $\Gamma_D = \partial\Omega$ and $\mathbf{H}|_{\partial\Omega} = \mathbf{H}^*$, by means of the integral equation method based on the Newton volume potential, we obtain [9]

$$\nabla\varphi(x) + \int\limits_{\Gamma_{\rm int}} ([\![\mathbf{n} \times \nabla\varphi]\!] \times \mathbf{V}^*(x,y) + [\![\mathbf{n} \cdot \nabla\varphi]\!]\mathbf{V}^*(x,y))dS_y =$$

$$= -\int\limits_{\Gamma_{\rm int}} ([\![\mathbf{n} \times \mathbf{w}]\!] \times \mathbf{V}^*(x,y) + [\![\mathbf{n} \cdot \mathbf{w}]\!]\mathbf{V}^*(x,y))dS_y -$$

$$- \int\limits_{\partial\Omega} (\mathbf{n} \times \mathbf{H}^*) \times \mathbf{V}^*(x,y) + (\mathbf{n} \cdot \mathbf{H}^*)\mathbf{V}^*(x,y)) dS_y +$$

$$+ \sum_{\Omega_k \in T_h} \int\limits_{\Omega_k} (\tilde{g}\mathbf{V}^*(x,y) + \mathbf{G} \times \mathbf{V}^*(x,y)) d\Omega_y, \quad x \in \Omega_k \in T_h.$$

Note that it is possible to use the integral equation based on Green's formula with fundamental solution [4]. Hovewer, these approaches can be expensive on computational work. Consider the least square method from [9]. We have

$$\sum_{(\partial\Omega_k \cap \partial\Omega) \in T_h} \int\limits_{(\partial\Omega_k \cap \partial\Omega)} \nabla\varphi \cdot \nabla\psi dS + \sum_{\Gamma_{kl} \in \Gamma_{\text{int}}} \left(\int\limits_{\Gamma_{kl}} [\![\nabla_\tau \varphi]\!] \cdot [\![\nabla_\tau \psi]\!] dS + \right.$$

$$\left. + \int\limits_{\Gamma_{kl}} [\![\mathbf{n} \cdot \nabla\varphi]\!] \cdot [\![\mathbf{n} \cdot \nabla\psi]\!] dS \right) = - \sum_{(\partial\Omega_k \cap \partial\Omega) \in T_h} \int\limits_{(\partial\Omega_k \cap \partial\Omega)} (\mathbf{w} - \mathbf{H}^*) \cdot \nabla\psi dS -$$

$$- \sum_{\Gamma_{kl} \in \Gamma_{\text{int}}} \left(\int\limits_{\Gamma_{kl}} [\![\mathbf{w}_\tau]\!] \cdot [\![\nabla_\tau \psi]\!] dS + \int\limits_{\Gamma_{kl}} [\![\mathbf{n} \cdot \mathbf{w}]\!] \cdot [\![\mathbf{n} \cdot \nabla\psi]\!] dS \right). \quad (4)$$

Here, ψ is a harmonic basis function [9]. Equation (4) was investigated in [9]. Usual estimates for h-convergence of approximate solutions [7] were also proved in [9].

Then consider the discontinuous Galerkin method [6] for solving (2) with our assumptions. We have the following scheme:

$$\sum_{\Omega_k \in T_h} \int\limits_{\Omega_k} \nabla\varphi \cdot \nabla\psi d\Omega - \sum_{\Gamma_{kl} \in \Gamma_{\text{int}}} \left(\int\limits_{\Gamma_{kl}} ([\![\psi]\!] \cdot \{\{\mathbf{n} \cdot \nabla\varphi\}\} + [\![\varphi]\!] \cdot \{\{\mathbf{n} \cdot \nabla\psi\}\}) dS + \right.$$

$$\left. + \int\limits_{\Gamma_{kl}} \beta [\![\varphi]\!] \cdot [\![\psi]\!] dS \right) + \sum_{\Gamma_{kl} \in (\Gamma_{\text{int}} \cup \partial\Omega)} \int\limits_{\Gamma_{kl}} [\![\mathbf{n} \times \nabla\varphi]\!] \cdot [\![\mathbf{n} \times \nabla\psi]\!] dS =$$

$$= - \sum_{\Omega_k \in T_h} \int\limits_{\Omega_k} (\psi \cdot g - \nabla\psi \cdot \mathbf{w}) d\Omega + \sum_{\Gamma_{kl} \in \Gamma_{\text{int}}} \int\limits_{\Gamma_{kl}} ([\![\psi]\!] \cdot \{\{\mathbf{n} \cdot \mathbf{w}\}\} +$$

$$+ [\![\mathbf{n} \cdot \mathbf{w}]\!] \cdot \{\{\psi\}\}) dS - \sum_{\Gamma_{kl} \in \partial\Omega} \int\limits_{\Gamma_{kl}} \psi \cdot (\mathbf{n} \cdot (\mathbf{H}^* - \mathbf{w})) dS +$$

$$+ \sum_{\Gamma_{kl} \in (\Gamma_{\text{int}} \cup \partial\Omega)} \int\limits_{\Gamma_{kl}} ([\![\mathbf{n} \times (\mathbf{H}^* - \mathbf{w})]\!] \cdot [\![\mathbf{n} \times \nabla\psi]\!]) dS,$$

where $\beta = \beta(x)$ is a penalty function [6]. Here, in standard scheme we include the conditions which provide continuity of $\mathbf{n} \times \mathbf{H}$ and $\mathbf{w}$ on $\Gamma_{\text{int}} \cup \partial\Omega$.

There is a second approach to apply the discontinuous Galerkin method for solving (2). Assume that it is possible to differentiate the equations of system (2). Then, instead of (2), we consider the problem

$$-\nabla^2 \mathbf{H} = \nabla \times \mathbf{G} - \nabla g, \quad x \in \Omega; \quad \mathbf{H} = \mathbf{H}^*, \quad x \in \partial\Omega.$$

For each harmonic component $u_i = \partial\varphi/\partial x_i$ of unknown vector $\mathbf{H} = \mathbf{u} + \mathbf{w}$, we have

$$\sum_{\partial\Omega_k \in T_h} \int\limits_{\Omega_k} \nabla u_i \cdot \nabla v d\Omega - \sum_{\Gamma_{kl} \in (\Gamma_{\text{int}} \cup \partial\Omega)} \left(\int\limits_{\Gamma_{kl}} (\llbracket v \rrbracket \cdot \{\{\mathbf{n} \cdot \nabla u_i\}\} + \right.$$

$$\left. + \llbracket u_i \rrbracket \{\{\mathbf{n} \cdot \nabla v\}\}) dS + \int\limits_{\Gamma_{kl}} \beta \cdot \llbracket u_i \rrbracket \cdot \llbracket v \rrbracket dS \right) =$$

$$= - \sum_{\Omega_k \in T_h} \int\limits_{\Omega_k} v \cdot ((\nabla \times \mathbf{G})_i - \partial g/\partial x_i) d\Omega -$$

$$- \sum_{\Gamma_{kl} \in \partial\Omega} \int\limits_{\Gamma_{kl}} ((\mathbf{n} \cdot \nabla v) \cdot (H_i^* - w_i) - \beta \cdot v \cdot (H_i^* - w_i)) dS -$$

$$- \sum_{\Gamma_{kl} \in (\Gamma_{\text{int}} \cup \partial\Omega)} \int\limits_{\Gamma_{kl}} (\llbracket v \rrbracket \cdot \{\{\mathbf{n} \cdot \nabla w_i\}\} + \llbracket w_i \rrbracket \cdot \{\{\mathbf{n} \cdot \nabla v\}\}) dS. \quad (5)$$

Here, $\beta = \beta(x)$ is a penalty function. We will use this approach in Section 4.

3.2. Numerical Example of Convergence. We investigate the experimental order of convergence (EOC) [6] for the least square method with harmonic basis for vector function (LSTV) in formulation (4) and also for the discontinuous Galerkin method (SIPG variant with harmonic basis) in formulation (5). Consider the model problem in $\Omega = (0, 2)^3$:

$$\nabla \cdot \mathbf{u} = 0, \quad \nabla \times \mathbf{u} = 0, \quad x \in \Omega; \quad \mathbf{u} = \mathbf{u}^*, \quad x \in \partial\Omega,$$

where $\mathbf{u}^*$ is a gradient of harmonic polynomial of the thirteenth order in spherical coordinates $x = (r, \theta, \phi)$:

$$\mathbf{u}^* = \nabla((r/3)^{13} \cdot (\sin(2\phi) \cdot C_{13,2} \cdot P_{13}^2(\cos(\theta)) + \\ + \cos(3\phi) \cdot C_{13,3} \cdot P_{13}^3(\cos(\theta)))),$$

where $P_n^m(\cos(\theta))$ is the associated Legendre function and $C_{n,m} = (2n+1)(n-k)!/(n+k)!$.

In accordance with [9, 10], in each cell Ω_k an unknown solution is sought in the form

$$\mathbf{u}(x)|_{\Omega_k} = \sum_{i=2}^{m(p_k)} c_{i-1}^{(k)} \nabla f_i^{(k)}(\xi), \tag{6}$$

where $f_i^{(k)}(\xi)$ is a harmonic basis function, $\xi = (\xi_1, \xi_2, \xi_3)$ is a point in local coordinate system, $\xi_n = (x_n - y_n^{(k)})/r^{(k)}$, $y_n^{(k)}$ is a coordinate of the center of the cell Ω_k, $n = 1, 2, 3$, $r^{(k)}$ is one half of the diameter h_k of Ω_k, $m(p_k)$ is a number of polynomials of degree $\leqslant p_k$, $c_i^{(k)}$ is an unknown coefficient. As harmonic basis f_j, $j = 1, \ldots, m$, we choose functions from the sequence

$$1; a_{2,1}; a_{2,2}; b_{2,2}; a_{3,1}; a_{3,2}; b_{3,2}; a_{3,3}; b_{3,3}; a_{4,1}; a_{4,2}; b_{4,2}; a_{4,3}; b_{4,3}; a_{4,4}; b_{4,4}; \ldots,$$

and these functions are computed by the recursion relations, which limit growth of round-off errors [10]:

$$a_{n+1,1} = \frac{2n+1}{n}\left(\xi_3 a_{n,1} - |\xi|^2 \frac{n-1}{2n-3} a_{n-1,1}\right), \quad n = 2, 3, \ldots,$$

$$a_{1,1} = 1, a_{2,1} = 3\xi_3;$$

$$a_{n+1,n+1} = \frac{2n+1}{(2n-1)2n}(\xi_1 a_{n,n} - \xi_2 b_{n,n}), \quad n = 1, 2, \ldots,$$

$$a_{1,1} = 1, b_{1,1} = 0.;$$

$$b_{n+1,n+1} = \frac{2n+1}{(2n-1)2n}(\xi_2 a_{n,n} + \xi_1 b_{n,n}), \quad n = 1, 2, \ldots,$$

$$a_{1,1} = 1, b_{1,1} = 0.;$$

$$a_{n+1,k+1} = \frac{2n+1}{n+k}\left(\frac{1}{2n-1}(\xi_1 a_{n,k} - \xi_2 b_{n,k}) + \frac{n-k}{2n-1}\xi_3 a_{n,k+1}\right),$$

$$n = 2, 3, \ldots, \quad k = 1, \ldots, n-1;$$

$$b_{n+1,k+1} = \frac{2n+1}{n+k}\left(\frac{1}{2n-1}(\xi_2 a_{n,k} + \xi_1 b_{n,k}) + \frac{n-k}{2n-1}\xi_3 b_{n,k+1}\right),$$

$$n = 2, 3, \ldots, \quad k = 1, \ldots, n-1.$$

Let e_h be the $L^2(\Omega)$-norm of an error of the solution on a mesh with the cells having a diameter h. If we assume that

$$e_h \approx C \cdot h^{\mathrm{EOC}},$$

Table 1. h- and p-convergence of LSTV and SIPG methods with harmonic basis in $L^2(\Omega)$-norm

Parameters		LSTV			SIPG			
h	n/m	p	e_h	EOC	p	e_h	EOC	β
$\sqrt{3}/2$	576/9		2.6138e-2			1.0863e-2		17
$\sqrt{3}/4$	4608/9	1	7.7298e-3	1.76	2	1.4974e-3	2.86	33
$\sqrt{3}/8$	36864/9		2.0555e-3	1.91		1.8805e-4	2.99	66
$\sqrt{3}/2$	1024/16		1.0060e-2			2.5528e-3		20
$\sqrt{3}/4$	8192/16	2	1.3968e-3	2.85	3	1.7425e-4	3.87	35
$\sqrt{3}/8$	65536/16		1.7772e-4	2.97		1.1004e-5	3.99	67
$\sqrt{3}/2$	1600/25		2.3093e-3			4.2100e-4		25
$\sqrt{3}/4$	12800/25	3	1.5681e-4	3.88	4	1.4301e-5	4.88	44
$\sqrt{3}/8$	102400/25		9.9338e-6	3.98		4.5265e-7	4.98	78
$\sqrt{3}/2$	2304/36		3.5790e-4			5.7223e-5		29
$\sqrt{3}/4$	18432/36	4	1.2318e-5	4.86	5	9.5903e-7	5.90	55
$\sqrt{3}/8$	147456/36		3.9267e-7	4.97		1.5079e-8	5.99	102
$\sqrt{3}/2$	3136/49		5.0943e-5			5.4686e-6		31
$\sqrt{3}/4$	25088/49	5	8.6722e-7	5.88	6	4.6431e-8	6.87	57
$\sqrt{3}/8$	200704/49		1.3864e-8	5.97		3.7082e-10	6.97	104
$\sqrt{3}/2$	4096/64	6	5.3294e-6		7	3.7498e-7		32
$\sqrt{3}/4$	32768/64		4.3950e-8	6.92		1.5758e-9	7.89	61
$\sqrt{3}/2$	5184/81	7	3.5386e-7		8	1.9958e-8		35
$\sqrt{3}/4$	41472/81		1.4272e-9	7.95		4.1696e-11	8.90	66
$\sqrt{3}/2$	6400/100	8	1.9218e-8		9	9.2338e-10		40
$\sqrt{3}/4$	51200/100		3.8491e-11	8.96		9.4132e-13	9.94	76
$\sqrt{3}/2$	7744/121	9	8.5297e-10		10	2.9282e-11		48
$\sqrt{3}/4$	61952/121		8.4414e-13	9.98		1.4300e-14	11.00	88
$\sqrt{3}/2$	9216/144	10	2.7879e-11		11	5.9665e-13		49
$\sqrt{3}/4$	73728/144		1.3724e-14	10.99		1.1026e-15		95

where C is independent of h, then for two meshes with cells of diameters h_1 and h_2, we have

$$\mathrm{EOC} \approx \frac{\log\left(e_{h_1}/e_{h_2}\right)}{\log\left(h_1/h_2\right)}.$$

Table 1 presents EOC for LSTV and SIPG with harmonic basis for the considered model problem. Here, p is the degree of harmonic basis and n is the number of equations. The obtained results are in a good agreement with theoretical estimations [9].

4. NUMERICAL COMPARISON OF METHODS ON MODEL MAGNETOSTATIC PROBLEM

Calculation of magnetic fields in large regions can be a challenge. The magnetic system of a physical experiment (for example, ALICE [11], PANDA [12] and, perhaps, some future experiments) may contain a huge solenoid with ferromagnetic screen and a large dipole with ferromagnetic core, i.e., the electromagnets having differently directed fields. To estimate the field behavior between two magnets, it is possible to use linear models without ferromagnetic parts (Figs. 1

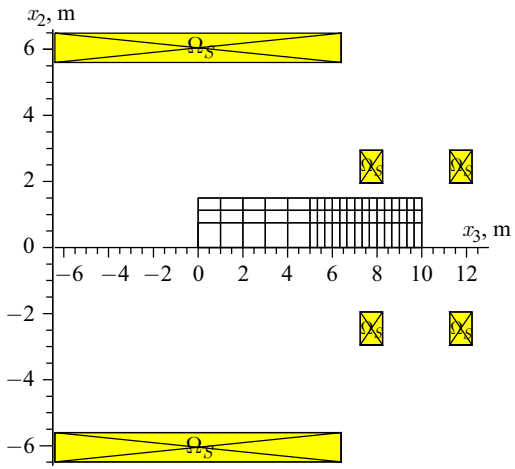

Fig. 1. Model of magnet system with two large solenoids and first calculation mesh in plane $x_1 = 0$

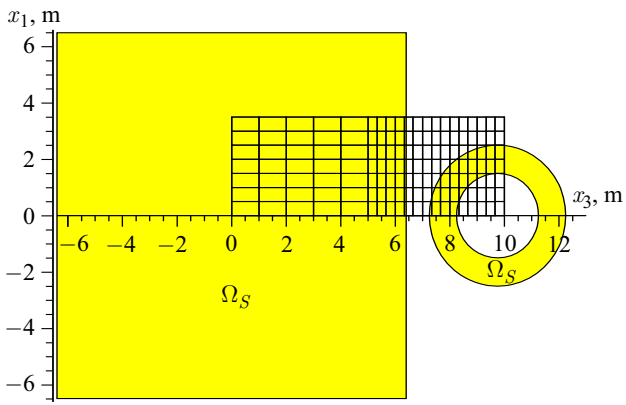

Fig. 2. Model of magnet system with two large solenoids and first calculation mesh (top view)

and 2). Such a model problem can be used for comparison of efficiency of the above-presented methods with harmonic basis. Let the Dirichlet problem for vector Laplace equation be solved in the region $\Omega = \{x = (x_1, x_2, x_3) : 0 < x_1 < 3.5; 0 < x_2 < 1.5; 0 < x_3 < 10.\}$ with condition $\mathbf{n} \times \mu_0 \mathbf{H}^*|_{\partial\Omega} = \mathbf{B}_\tau^S$ or $\mu_0 \mathbf{H}^*|_{\partial\Omega} = \mathbf{B}^S$. Here, $\mathbf{B}^S$ is the total field of two solenoids computed by the Biot–Savart law [13] with given current densities providing $B_3(0) = 0.5$ T and $B_2(0, 0, 9.75) = 0.75$ T for the horizontal and the vertical solenoid, respectively. Figures 3 and 4 show the behavior of the field between the magnets in two perpendicular planes.

We have solved this problem by the least square method with harmonic basis for vector function (LSTV) in formulation (4), the discontinuous Galerkin method (SIPG variant [6]) in formulation (5) and the continuous Galerkin method (CG) [7] in the same assumptions as for SIPG method.

The results obtained with the above-mentioned methods are presented in Tables 2–4, where we have introduced the following notation: CG27 and CG64 are the CG method with 27- and 64-noded elements in the form of hexahedrons [7, 14], respectively; LSTV-1 is LSTV with the boundary condition $\mathbf{n} \times \mathbf{B}^*|_{\partial\Omega} = \mathbf{B}_\tau^S$, LSTV-2 is LSTV with the boundary condition $\mathbf{B}|_{\partial\Omega} = \mathbf{B}^S$; "nelm", p, n, m are the number of elements, the maximal degree of basis functions, the total number of unknowns (freedom degrees), and the number of unknowns in each element, respectively; $\delta = \max_{x \in \Omega_h} |\mathbf{B}^* - \mathbf{B}_h|/|\mathbf{B}^*|$, where Ω_h is the grid of $56 \times 24 \times 160$ points uniformly dividing the region Ω; δ^* means the same as δ,

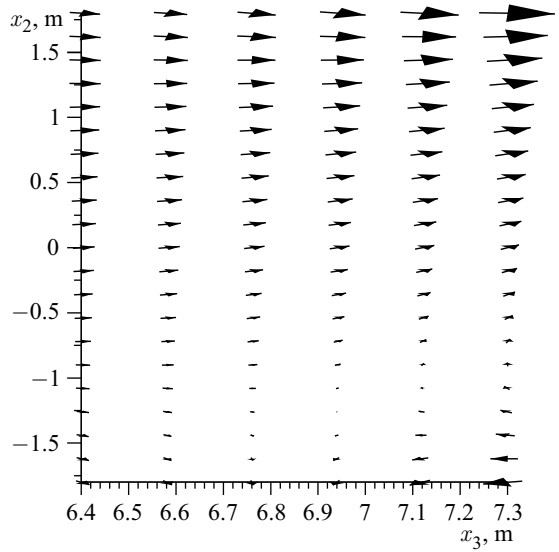

Fig. 3. Distribution of total magnetic flux density between the magnets in plane $x_1 = 0$

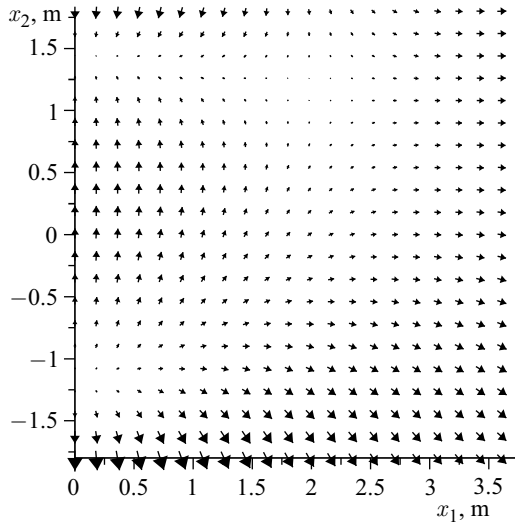

Fig. 4. Distribution of total magnetic flux density between the magnets in plane $x_3 = 6.825$ m

Table 2. h- and p-convergence of SIPG method with harmonic basis

p	nelm	n/m	δ	it/iter+	β
2	420	3780/9	9.7048e-3	89/27	0.2
	3360	30240/9	1.6221e-3	148/45	0.3
	26880	241920/9	2.3418e-4	282/85	0.6
3	420	6720/16	2.1110e-3	108/30	0.3
	3360	53760/16	1.9813e-4	148/45	0.3
	26880	430080/16	1.6585e-5	282/84	0.6
4	420	10500/25	4.9070e-4	100/28	0.25
	3360	84000/25	3.6785e-5	180/50	0.45
	26880	672000/25	1.6499e-6	323/91	0.8

and $\mathbf{B}_h$ is computed in each element with the help of harmonic interpolation formulas. By "it", "iter" and "iter+" we denote the number of iterations when using the conjugate gradient method with a block-diagonal preconditioner [15], the method ICCG(0) [15] and ICCG(0) with a block-diagonal preconditioner, respectively. Here each block corresponds to element matrix. It is important to note that the number of iterations of the preconditioned conjugate gradient method is approximately in proportion to the square root of the condition number of a matrix [15].

Table 2 shows h- and p-convergence of SIPG method with the harmonic basis. The first adaptive mesh is depicted in Figs. 1 and 2. Each consequent mesh

Table 3. h- and p-convergence of CG method

Type	nelm	n/m	δ	δ^*	iter
CG27	420	4305/27	3.0317e-3	2.3799e-3	13
	3360	30537/27	4.1259e-4	2.0613e-4	23
	26880	229425/27	**2.2415e-5**	8.9953e-6	43
CG64	420	10060/64	3.4268e-4	1.1293e-4	13
	3360	71977/64	1.5569e-5	4.8405e-6	24
	26880	542905/64	**1.1001e-6**	3.5730e-7	44

Table 4. h- and p-convergence of LSTV methods

Parameters			LSTV-1		LSTV-2	
p	nelm	n/m	δ	it/iter+	δ	it/iter+
2	420	3780/9	7.0005e-2	78/28	5.1976e-2	54/20
	3360	30240/9	1.9773e-2	150/53	1.6604e-2	102/37
	26880	241920/9	5.3522e-3	286/102	4.6155e-3	192/70
3	420	6720/16	1.2205e-2	81/28	1.1856e-2	56/20
	3360	53760/16	2.2320e-3	151/51	2.0022e-3	103/36
	26880	430080/16	3.1810e-4	286/98	2.8910e-4	193/68
4	420	10500/25	3.1465e-3	81/28	2.8916e-3	56/21
	3360	84000/25	3.2983e-4	151/52	3.0555e-4	103/37
	26880	672000/25	2.6755e-5	286/99	2.3730e-5	193/69
5	420	15120/36	7.2374e-4	81/29	6.4707e-4	56/21
	3360	120960/36	4.9031e-5	152/53	4.2319e-5	104/37
	26880	967680/36	2.3698e-6	286/102*	1.9520e-6	193/70*
6	420	20580/49	1.7649e-4	81/29	1.7323e-4	56/21
	3360	164640/49	**6.9802e-6**	152/54	**6.8604e-6**	103/38
	26880	1317120/49	2.1848e-7	287/102*	1.8235e-7	193/70*
7	420	26880/64	5.7201e-5	81/29	5.9091e-5	56/22
	3360	215040/64	**1.3093e-6**	152/54	**1.4861e-6**	103/38
8	420	34020/81	2.1388e-5	81/29	2.0118e-5	56/22
9	420	42000/100	6.6198e-6	81/30	6.1836e-6	57/22

is obtained by dividing each element from the previous mesh into eight identical parts. The parameter β is chosen from the set $\{0.1, 0.15, 0.2, \ldots, 0.9\}$ to obtain a minimal value of δ. For CG64 (Table 3) we have used "static condensation", i.e., elimination unknowns, corresponding to inner nodes of elements, from the system. To calculate the volume integrals, the product of three- or four-point one-dimensional Gauss formulas for each direction of integration is used. In LSTV (Table 4), for integration, the special two-dimensional 17-noded formulas [16] with a minimum number of nodes are used.

Calculations and analysis of the tables show that, in comparison with SIPG, in LSTV the required accuracy is achieved by increase in degree of basis functions at unit. But in LSTV the same accuracy is reached faster than in SIPG. Concerning the CG method it should be noted that basis functions in the form of tensor product contain monomials up to degree 6 (CG27) and up to degree 9 (CG64). However, in LSTV the same accuracy can be reached on a coarser mesh, but with more filled matrix. In the tables the compared results are marked in bold type. Note that the number of iterations for LSTV weakly depends on p. Here, 102^* and 70^* are estimating values. Table 4 also shows the possibility of using high-order harmonic basis in LSTV for solving problems with smooth solutions on meshes with small numbers of elements.

5. APPLICATION OF HIGH-ORDER HARMONIC BASIS FOR SOLVING NONLINEAR MAGNETOSTATIC PROBLEMS

As is well known, in adaptive approach the usual $C^{(0)}$ continuous finite element basis [7] requires that additional elements and nodes be generated or additional computational work be carried out for processing hanging nodes and edges. It is not required in projection methods with the discontinuous basis, presented in Section 4. The basis is very convenient for hp-adaptive problem solving with a high accuracy, allows one to increase easily a local order of approximation and to work with the meshes containing hanging nodes and edges. However, in this case, the multi-frontal parallel direct solver is required, for example, from KRYLOV library [17].

5.1. New Weak Formulations of the Nonlinear Magnetostatic Problem for Two Scalar Potentials. To solve the problem of magnetostatics in formulation (1), one usually presupposes that the function $\mu(|\nabla\varphi^{(1)}|)$ is a piecewise constant on each element in $\Omega^{(1)}$. It follows that for each such element the potential $\varphi^{(1)}$ is harmonic and it is possible to use harmonic basis of the first order for its finding. For this case, in the framework of the continuous Galerkin approach, the weak formulation for (1) was presented in [2]. But the formulation is not suitable for application of high-order harmonic basis. Therefore, we write our formulation in another way. Introduce the following notation:

$$[\![\varphi^{(i)}, \varphi^{(j)}, v^{(i)}, v^{(j)}]\!]|_{\Gamma_{k,l}} =$$

$$= \begin{cases} [\![\varphi^{(i)}]\!][\![v^{(i)}]\!] + [\![\mu^{(i)}\frac{\partial\varphi^{(i)}}{\partial n}]\!][\![\mu^{(i)}\frac{\partial v^{(i)}}{\partial n}]\!] + [\![\nabla_\tau\varphi^{(i)}]\!][\![\nabla_\tau v^{(i)}]\!], & x \in \Gamma_{k,l}, i = j; \\ (\varphi^{(i)} - \varphi^{(j)})(v^{(i)} - v^{(j)}) + \Big(\mu^{(i)}\frac{\partial\varphi^{(i)}}{\partial n} - \mu^{(j)}\frac{\partial\varphi^{(j)}}{\partial n}\Big)\Big(\mu^{(i)}\frac{\partial v^{(i)}}{\partial n} - \mu^{(j)}\frac{\partial v^{(j)}}{\partial n}\Big) + \\ \qquad + \nabla_\tau(\varphi^{(i)} - \varphi^{(j)}) \cdot \nabla_\tau(v^{(i)} - v^{(j)}), & x \in \Gamma_{k,l}, i \neq j. \end{cases}$$

In this notation we have

$$\sum_{k=1}^{2}\Bigg(\int\limits_{\Gamma_{\text{int}}^{(k)}}[\![\varphi^{(k)},\varphi^{(k)},v^{(k)},v^{(k)}]\!]dS+\int\limits_{\Gamma_D^{(k)}}\varphi^{(k)}v^{(k)}dS+$$

$$+\int\limits_{\Gamma_N^{(k)}}\mu^{(k)}\frac{\partial\varphi^{(k)}}{\partial n}\mu^{(k)}\frac{\partial v^{(k)}}{\partial n}dS\Bigg)+\int\limits_{\Gamma}[\![\varphi^{(1)},\varphi^{(2)},v^{(1)},v^{(2)}]\!]dS=$$

$$=\int\limits_{\Gamma}\Bigg(\varphi^{S}(v^{(1)}-v^{(2)})+\mu^{(2)}H_n^S\Bigg(\mu^{(1)}\frac{\partial v^{(1)}}{\partial n}-\mu^{(2)}\frac{\partial v^{(2)}}{\partial n}\Bigg)+$$

$$+\mathbf{H}_\tau^S\cdot\nabla_\tau(v^{(1)}-v^{(2)})\Bigg)dS. \quad (7)$$

Here, $\Gamma_{\text{int}}^{(k)}$ is the inner boundary between elements and $v^{(k)}$ is a weight function in the region $\Omega^{(k)}$, $k=1,2$. As a result of discretization, we have a symmetric matrix and a right side depending on $\mu^{(1)}$ and, hence, on the required solution.

5.2. Example of Solving the Nonlinear Magnetostatic Problem. An important question for electromagnets is about saturation of ferromagnetic parts [18]. To study this effect, at a magnet design stage, we need to solve nonlinear magnetostatic problems in order to obtain distribution of a module field in the ferromagnetic region. Figure 5 shows a symmetric part of the cross section by the center plane of a spectrometer magnet model. The considered model is investigated in [19]

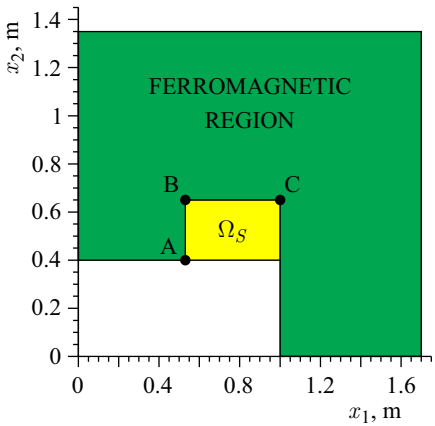

Fig. 5. Computational model of the electromagnet

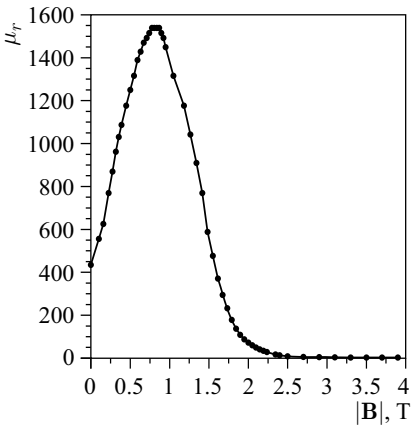

Fig. 6. Permeability μ_r versus $|\mathbf{B}|$

with the help of the continuous Galerkin approach in the framework of formulation (1) for 2D and 3D. It is assumed that the magnetic core is a magnetic isotropic medium. The behavior of the magnetic permeability μ_r depending on magnetic flux density $\mathbf{B}$ is shown in Fig. 6. The prescribed current density $\mathbf{J}_1$ provides $B_2(0) = 1.07$ T. The model contains singularities at points A, B, C, which influence saturation.

We solve the nonlinear magnetostatic problem in formulation (7), where the Neumann condition is given at $x_1 = 0$, and the Dirichlet condition at lines $x_2 = 0$, $x_1 = 3.7$, $x_2 = 3.35$, remote from the center. The harmonic basis of order $2, 3, \ldots, 10$ is used: $\varphi^{(k)}(x)|_{\Omega_i} = \sum\limits_{j=1}^{m(p_i)} c_j^{(i)} f_j^{(i)}(\xi)$. In the ferromagnetic region $p_i|_{\Omega^{(1)}} = 2$. For solving system (7), write the iterative process [20]:

$$\sum_{k=1}^{2}\Bigg(\int\limits_{\Gamma_{\text{int}}^{(k)}} [\![\varphi_{\text{nit}+1/2}^{(k)}, \varphi_{\text{nit}+1/2}^{(k)}, v^{(k)}, v^{(k)}]\!] dS + \int\limits_{\Gamma_D^{(k)}} \varphi_{\text{nit}+1/2}^{(k)} v^{(k)} dS +$$

$$+ \int\limits_{\Gamma_N^{(k)}} \mu_{\text{nit}}^{(k)} \frac{\partial \varphi_{\text{nit}+1/2}^{(k)}}{\partial n} \mu_{\text{nit}}^{(k)} \frac{\partial v^{(k)}}{\partial n} dS \Bigg) + \int\limits_{\Gamma} [\![\varphi_{\text{nit}+1/2}^{(1)}, \varphi_{\text{nit}+1/2}^{(2)}, v^{(1)}, v^{(2)}]\!] dS =$$

$$= \int\limits_{\Gamma} \Bigg(\varphi^S (v^{(1)} - v^{(2)}) + \mu^{(2)} H_n^S \left(\mu_{\text{nit}}^{(1)} \frac{\partial v^{(1)}}{\partial n} - \mu^{(2)} \frac{\partial v^{(2)}}{\partial n} \right) + \tag{8}$$

$$+ \mathbf{H}_\tau^S \cdot \nabla_\tau (v^{(1)} - v^{(2)}) \Bigg) dS,$$

$$\varphi_{\text{nit}+1}^{(k)} = w_{\text{nit}} \cdot \varphi_{\text{nit}+1/2}^{(k)} + (1 - w_{\text{nit}}) \cdot \varphi_{\text{nit}}^{(k)}, \quad k = 1, 2, \quad \text{nit} = 0, 1, 2, \ldots,$$

where $\varphi_0^{(k)}$ is given, w_{nit} is a parameter, $w_0 = 1$, at $\text{nit} > 0$ it is adaptively chosen as function of the variable

$$\sigma_{\text{nit}} = \left(\int\limits_{\Omega^{(1)}} |\mu_{\text{nit}}^{(1)} - \mu_{\text{nit}-1}^{(1)}| / \mu_{\text{nit}}^{(1)} d\Omega \right) \Bigg/ \int\limits_{\Omega^{(1)}} d\Omega.$$

System (8), corresponding to an adaptive mesh with numerous hanging nodes, is solved by a direct method in each iteration step on nonlinearity. Here, use of KRYLOV library [17] is possible.

We executed computations for the sequence of current densities $\mathbf{J}_1$, $\mathbf{J}_1 \cdot 0.75$, $\mathbf{J}_1 \cdot 0.5$ and $\mathbf{J}_1 \cdot 0.25$ on the same mesh and at the same distribution of an order of approximation. Figure 7 shows a typical convergence of σ_{nit}. Table 5 presents

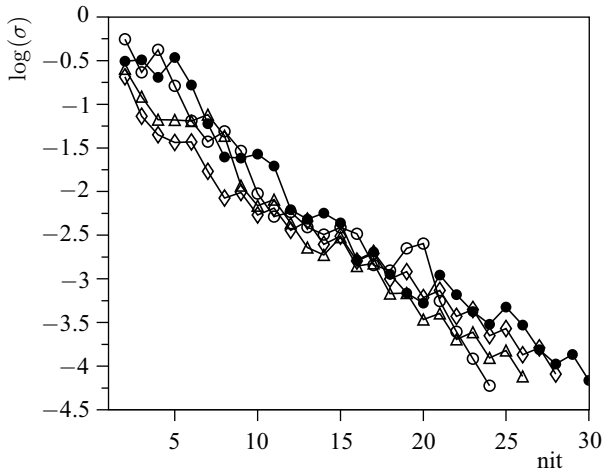

Fig. 7. Typical convergence of σ_{nit}: $\diamond$, $\triangle$, $\bullet$, $\circ$ for current density $\mathbf{J}_1$, $\mathbf{J}_1 \cdot 0.75$, $\mathbf{J}_1 \cdot 0.5$, and $\mathbf{J}_1 \cdot 0.25$, respectively

Table 5. The field module peak and the field in the magnet center

Field	$\mathbf{J}_1$	$\mathbf{J}_1 \cdot 0.75$	$\mathbf{J}_1 \cdot 0.5$	$\mathbf{J}_1 \cdot 0.25$
$\max \lvert\mathbf{B}\rvert$, T	2.5415	2.2875	1.8883	1.4816
$B_2(0,0)$, T	1.0689	0.8047	0.5373	0.2682

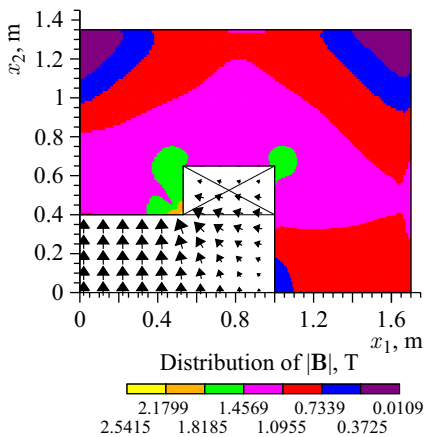

Fig. 8. Field behavior obtained by means of high-order harmonic basis for current density $\mathbf{J_1}$

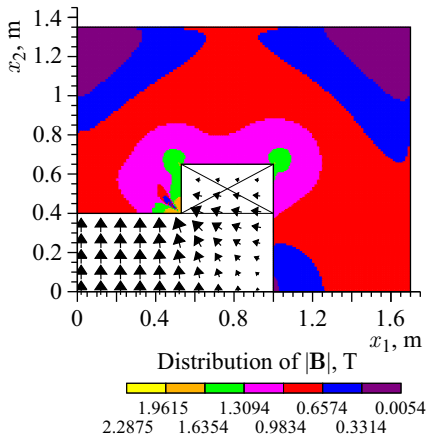

Fig. 9. Field behavior obtained by means of high-order harmonic basis for current density $\mathbf{J}_1 \cdot 0.75$

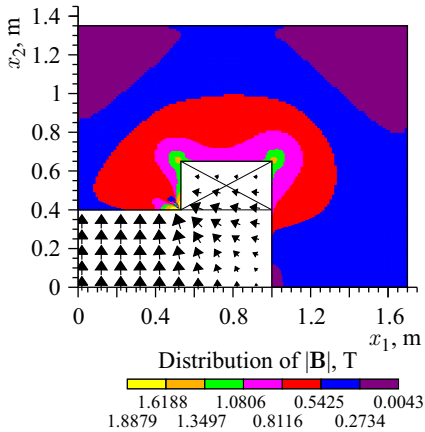

Fig. 10. Field behavior obtained by means of high-order harmonic basis for current density $\mathbf{J}_1 \cdot 0.5$

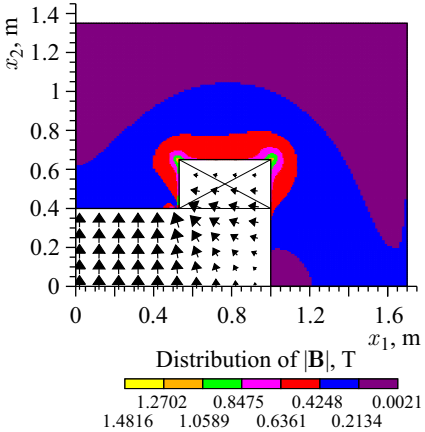

Fig. 11. Field behavior obtained by means of high-order harmonic basis for current density $\mathbf{J}_1 \cdot 0.25$

convergence of field module peak in the ferromagnetic material and the main field component in the magnet center for different current densities.

The distributions of field module in the ferromagnetic media and field behavior in the nonmagnetic region are presented in Figs. 8–11.

6. CONCLUSIONS AND FUTURE WORK

In this work we have considered the linear and nonlinear magnetostatic problems and have shown possibilities to use our high-order harmonic basis for their solving. For the nonlinear problem with respect to two scalar potentials, such a basis is used in nonmagnetic medium. Comparison with the continuous Galerkin method and with the considered discontinuous methods of a high order at various h and p, for 3D model linear problems, shows that the harmonic basis is especially effective on adaptive meshes. For solving the nonlinear magnetostatic problem, the new weak formulation, obtained by the authors, was used. Using the numerical example it is shown that the formulation keeps the monotonicity property of the considered magnetostatic problem even with hanging nodes.

In the paper [21], the special algorithm for discretization of the discontinuous Galerkin method is presented, where high degree of convergence of approximate solutions was theoretically proved in the case of linear problems with singularities. But as Figs. 8–11 show, for accounting singularities in points A, B, C it is necessary to use similar algorithms for discretizations of projection discontinuous methods in both nonmagnetic and magnetic medium.

REFERENCES

1. The Large Hadron Collider. CERN/AC/95-05 (LHC) / Eds. P. Lefèvre, T. Pettersson, Geneva, 1995.
2. *Simkin J., Trowbridge C. W.* Three Dimensional Non-Linear Electromagnetic Field Computations Using Scalar Potentials // Proc. IEE. 1980. V. 127. Pt. B, No. 6. P. 368–374.
3. *Zhidkov E. P., Yuldashev O. I., Yuldasheva M. B.* An Adaptive Algorithm for Computing a Function on the Lipschitzian Boundary of a Three-Dimensional Solid Based on a Prescribed Gradient and Its Application in Magnetostatics // Comput. Math. Math. Phys. 2002. V. 42. P. 1764–1779.
4. *Brebbia C. A., Telles J. C. F., Wrobel L. C.* Boundary Element Techniques. Berlin: Springer, 1984.
5. *Bochev P. B., Gunzburger M. D.* Least-Squares Finite Element Methods. New York: Springer, 2009.
6. *Dolejší V., Feistauer M.* Discontinuous Galerkin Methods. Analysis and Applications to Compressible Flow. Springer Series in Computational Mathematics. New York: Springer, 2015.
7. *Ciarlet P.* The Finite Element Method for Elliptic Problems. Amsterdam: North-Holland, 1978.
8. *Bykhovsky E. B., Smirnov N. V.* On the Orthogonal Decompositions of the Space of Vector-Functions Which Are Squarely Summable over the Domain and on Operators of the Vector Analysis // Tr. MIAN SSSR. 1960. V. 59. P. 5–36 (in Russian).
9. *Yuldasheva M. B., Yuldashev O. I.* Boundary Least Squares Method with 3d Harmonic Basis of a High Order for Solving Linear Div-Curl Systems // Russ. J. Numer. Anal. Math. Modelling. 2017 (submitted).
10. *Yuldashev O. I., Yuldasheva M. B.* A Boundary Method of Weighted Residuals with Discontinuous Basis Functions for High-Accuracy Solving Linear Boundary Value Problems with Laplace's or Poisson's Equation // PFUR Bull.: Math., Inform. Sciences, Phys. 2013. V. 4. P. 18–28 (in Russian).
11. *Aamodt K. et. al. (ALICE collab.).* The ALICE Experiment at the CERN LHC // J. Instrum. 2008. V. 3, No. S08002. P. 1–260.
12. *Boca C.* The Experiment PANDA: Physics with Antiprotons at FAIR // EPJ Web Conf. 2015. V. 95, No. 01001. P. 1–7.
13. *Gyimesi M., Lavers D., Pawlak T., Ostergaard D.* Biot–Savart Integration for Bars and Arcs // IEEE Trans. Mag. 1993. V. 29. P. 2389–2391.
14. *Shaidurov V. V.* Multigrid Methods for Finite Elements. Dordrecht: Springer, 1995.
15. *van der Vorst H.* Iterative Krylov Methods for Large Linear Systems. Cambridge: Cambridge University Press, 2003.
16. *Mysovskih I. P.* Interpolation Cubature Formulas. Moscow: Nauka, 1981 (in Russian).
17. *Butyugin D. S., Il'in V. P., Perevozkin D. V.* Parallel Methods for SLAE Solving on the Systems with Distributed Memory in KRYLOV Library // SUrSU Bull.: Comput. Math. Informat. 2012. V. 306, No. 47. P. 22–36 (in Russian).

18. *Akishin P. G., Isupov A. Y., Khrenov A. N. et al.* Optimization of a Large Aperture Dipole Magnet for Baryonic Matter Studies at Nuclotron // Phys. Part. Nucl. Lett. 2015. V. 12, No. 2. P. 305–309.

19. *Davletshin R. I., Zhidkov E. P., Kulikov V. V., Ryltsov V. V., Yuldashev O. I., Yuldasheva M. B.* Computing Model of the Magnet for a Project of the Experiment with Polarized Target in ITEP. JINR Commun. P11-98-351. Dubna, 1998 (in Russian).

20. *Samarskii A. A., Nikolaev E. S.* Numerical Methods for Grid Equations. Vol. II: Iterative Methods. Basel: Birkhäuser, 1989.

21. *Schötzau D., Schwab C., Wihler T. P.* hp-DGFEM for Second Order Elliptic Problems in Polyhedra II: Exponential Convergence // SIAM J. Numer. Anal. 2013. V. 51. P. 2005–2035.

Received on September 28, 2017.

Редактор *Е. И. Кравченко*

Подписано в печать 10.11.2017.
Формат 60 × 90/16. Бумага офсетная. Печать офсетная.
Усл. печ. л. 1,31. Уч.-изд. л. 1,87. Тираж 215 экз. Заказ № 59264.

Издательский отдел Объединенного института ядерных исследований
141980, г. Дубна, Московская обл., ул. Жолио-Кюри, 6.
E-mail: publish@jinr.ru
www.jinr.ru/publish/